Ayyaz Ahmad*, Jianjia Liu, Xiaochi Liu, Li Li, Yisheng Xu and Xuhong Guo*

Synthesis of Ag$_2$O nano-catalyst in the spherical polyelectrolyte brushes and its application in visible photo driven degradation of dye

Abstract: Ag$_2$O nanoparticles (NPs) were synthesized using colloidal solution of spherical polyelectrolyte brushes (SPB) as nano-reactors. In this work, the average diameter of Ag$_2$O NPs was around 10 nm as determined by transmission electron microscopy (TEM). The composite NPs of Ag$_2$O immobilized in SPB (Ag$_2$O-SPB) showed significant absorption in the visible light region as confirmed by UV-Vis diffuse reflectance spectra (DRS), and their photoluminescence (PL) exhibited emission peak in the visible range. Ag$_2$O-SPB has shown outstanding photocatalytic activity during degradation of methyl blue (MB) in the visible light. This work will open up a new way to prepare ideal Ag$_2$O nano-catalyst for the remediation of wastewater using visible light.

Keywords: Ag$_2$O; spherical polyelectrolyte brush; visible photocatalyst.

1 Introduction

In the last century, industries have been grown rapidly. This rapid industralization, however, has generated large amount of pollutants which has created alarming situations for the environment and human health (1, 2). Dealing with these pollutants is becoming a big problem with the passage of time. It is well known that photocatalyst has been extensively used in the successful degradation of different kinds of pollutants present in the wastewater (3, 4). In order to make photocatalyst cost-effective and efficient, reseachers have exploited the visible light of the sun because the visible light consists of about 45% of solar light spectrum while UV light only has around 4% (5, 6). TiO$_2$ is the most extensively used photocatalyst for the treatment of organic waste but it can be activated in UV light due to its wide band gap of 3.2 eV (4, 7–10). Besides TiO$_2$, other photcatalysts include, for instance, ZnO, SnO$_2$, and ZrO$_2$, but they are also active in UV light due to their wide band gap (11–19). Several efforts have been made to utilize wide-band gap photocatalyst that could also be effective under visible light by doping it with some metal/non-metal or coupling with some narrow-band gap semi-conductors (4, 15, 20–23). Methylene blue is an organic dye which is used in leather, cotton fiber and as a biological stain. It is dangerous if consumed. It effects the humans by causing respiratory tract, skin and eye irritation (24).

Silver oxide (Ag$_2$O) with a narrow-band gap of about 1.2 eV has been employed as a highly efficient and stable photocatalyst. The Ag$_2$O photocatalyst is a promising candidate for the removal of hazardous organic materials from wastewater (25–27). Ag$_2$O has been employed in many industrial applications such as anti-bacterial activity, electrode material, and as cleaning agents (28–30). Due to its high catalytic activity and selectivity, Ag$_2$O has attracted the attention of many researchers (31, 32). As reported by Yu et al. and Wang et al., Ag$_2$O nanoparticles (NPs) as a visible light driven photocatalysts had exhibited self-stability during the photo-degradation process (26, 33).

On the other hand, NPs are required to be dispersed in the liquid phase. For that purpose, stabilizers are used to keep them dispersed stably in the liquid phase (34). However, NPs tend to aggregate in the absence of a stable system. Polymers have been widely used as a stabilizer in NP stabilization (35). Spherical polyelectrolyte brushes (SPB) consist of a spherical polymeric core, where linear

*Corresponding authors: Ayyaz Ahmad and Xuhong Guo, State Key Laboratory of Chemical Engineering, East China University of Science and Technology, Shanghai 200237, PR China,
Phone/Fax: +86 21 6425 3491,
e-mail: ayyazahmad@mail.ecust.edu.cn (A. Ahmad);
guoxuhong@ecust.edu.cn (X. Guo)
Ayyaz Ahmad: Department of Chemical Engineering, University of Gujrat, Pakistan
Xuhong Guo: Key Laboratory of Xinjiang Uygur Autonomous Region and Engineering Research Center of Xinjiang Bingtuan of Materials-oriented Chemical Engineering, Shihezi University, Xinjiang 832000, PR China
Jianjia Liu, Xiaochi Liu, Li Li and Yisheng Xu: State Key Laboratory of Chemical Engineering, East China University of Science and Technology, Shanghai 200237, PR China

polyelectrolyte (PE) chains are attached either by covalent bond or by physical adsorption (36, 37). The counterion concentration inside the SPB always remains constant because of the Donnan effect (38). Due to the confinement of these counter ions within brushes, SPB have proven to be well-defined and effective nanoreactors. If metal ions replace the counter ions confined within SPB, NPs can be generated by the reduction of these metal ions. NPs will be stabilized by SPB without addition of other stabilizers (35, 39–41).

Herein, we report the facile and simple synthesis of Ag$_2$O NPs in SPB nanoreactors. First, we synthesized the poly(acrylic acid) (PAA) brushes, having carboxylic groups, attached to the polystyrene (PS) core. Then, H$^+$ ions of carboxylic group were exchanged with silver ions. Finally, Ag$_2$O NPs formed after the addition of NaOH in the mixture, as shown in the schematic diagram (Figure 1). The Ag$_2$O NPs remains very stable in the dispersion of SPB for a long time. The composite NPs of Ag$_2$O immobilized in SPB (Ag$_2$O-SPB) showed outstanding photocatalytic activity during degradation of methyl blue (MB) in the visible light. This study opens up a new approach to prepare invisible photo-droven Ag$_2$O nano-catalyst for dye wastewater treatment.

2 Experimental section

2.1 Materials

Potassium peroxodisulfate (KPS), styrene, sodium hydroxide and acrylic acid were obtained from Shanghai Lingfeng Chemical Reagent Co., Ltd. Sodium dodecylsulfate (SDS) was obtained from Shanghai Reagent Company (Shanghai, China). The initiator KPS was purified by re-crystallization in water prior to use and stored in refrigerator. SDS and the monomers were purified by reduced pressure distillation to remove inhibitor. Silver nitrate (AgNO$_3$) was purchased from Sinopharm Chemical Research Co., Ltd. (Beijing, China). The water used in the experiment was purified with the help of a Millipore Milli-Q system. All reagents have been
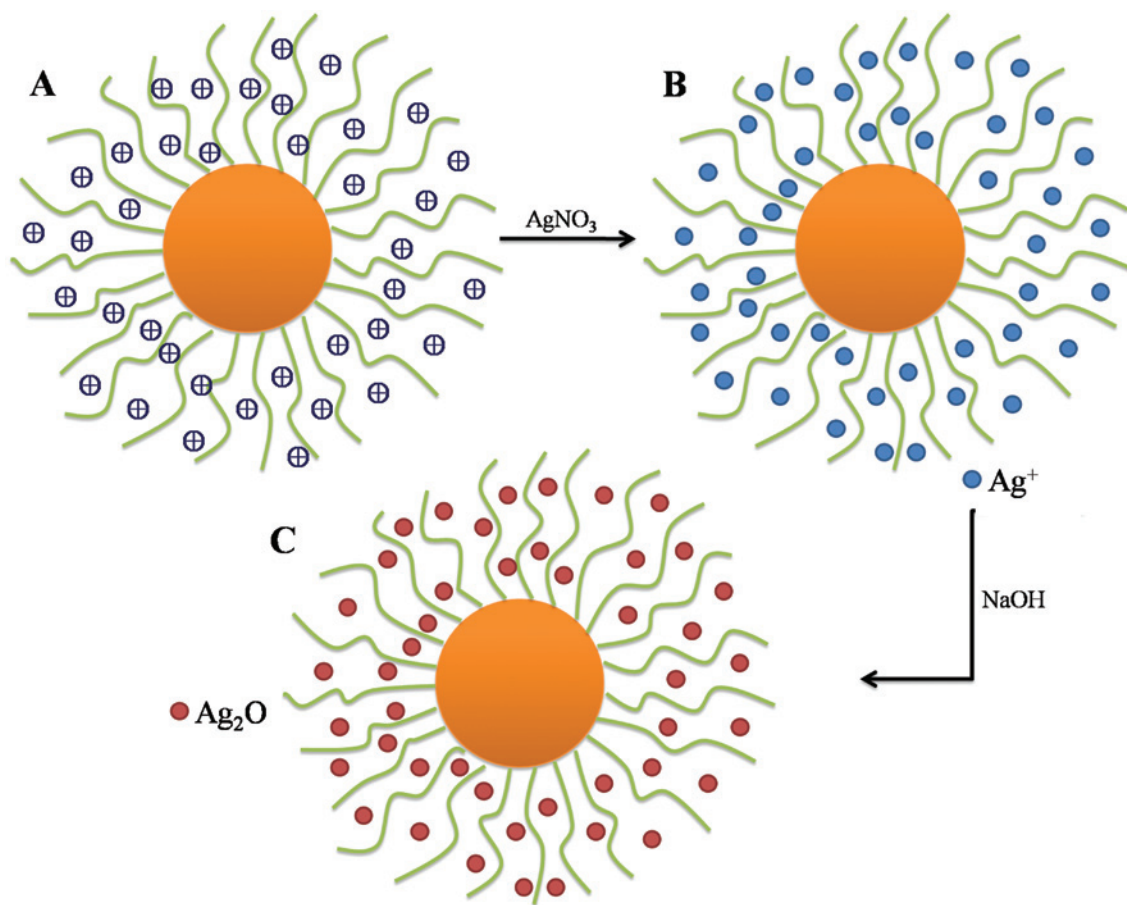
Figure 1: Schematic representation of Ag$_2$O synthesis on SPB (A) SPB (B) Ag$^+$ ions replacing the counter ions by the addition of AgNO$_3$, (C) Ag$_2$O NPs synthesis by adding the NaOH.

purchased from different companies (names are given in Materials section) within China.

2.2 Synthesis of spherical polyelectrolyte brushes

The 2-[p-(2-hydroxy-2-methylpropiophenone)]-ethylene-glycol-methacrylate (HMEM), photo initiator was prepared according to method reported in our previous paper (36). The PS core was synthesized by conventional radical polymerization. Briefly, 2.0 g of styrene was mixed with 0.05 g of SDS and 0.12 g of KPS. Before the start of reaction, the whole reactor was degassed by repeated evacuation and subsequent injection of nitrogen. The mixture was then heated to 80°C with vigorous stirring for 2 h. Then, 0.02 g of photo initiator dissolved in 1.8 g acetone was added under starved conditions (0.05 ml/min). A thin shell of photo initiator layer was generated on the surface of PS core. The latex was cooled to room temperature and purified by serum replacement against pure water until the conductivity of eluate keeps constant.

PS core latex (1 wt%) was mixed with an appropriate amount of acrylic acid (100%) in a homemade UV photo reactor. The reactor was degassed by repeated evacuation and subsequent injection of N$_2$. The photo-emulsion polymerization was carried out under the radiation of UV light (150 W) at room temperature. The obtained SPB colloid was purified by dialysis against the water.

2.3 Synthesis of Ag$_2$O NPs in SPB

For the synthesis of Ag$_2$O NPs, 5 ml of SPB (1 wt%) was dispersed in 40 ml water in three round neck bottom flask. Two milliliter of a 62.5 mM solution of AgNO$_3$ was added at the controlled rate by micro syringe to the SPB dispersion to make the total concentration of AgNO$_3$ at 2.6 mM in the solution and stirred for 2 h to exchange H$^+$ with Ag$^+$ under a nitrogen environment. Then 2 ml of equimolar aqueous sodium hydroxide solution was added to the above mixture dropwise at the feeding rate of 0.1 ml/min at 50°C. The reaction was carried out for further 2 h. The SPB/Ag$_2$O composite was then cooled down at room temperature and purified afterwards by dialysis against the pure water.

2.4 Characterization

Using the particle sizing system of NICOMP 380 ZLS at a fixed scattering angle of 90°, dynamic light scattering (DLS) was used to determine the hydrodynamic size of particles. The transmission electron microscopy (TEM) was performed using a JEOL-2100 electron microscope operating at 200 kV. To study the interaction between the Ag$_2$O and SPB, the Fourier transmission infrared (FTIR) spectra was performed using a 6700 Fourier transform spectrometer (Thermo Nicolet Corp.). The UV-Vis diffuse reflectance spectra (UV-Vis DRS) for the dry-pressed disk catalyst samples were obtained using a scan UV-Vis spectrophotometer (Varian, Cary 500) fitted with an integrating sphere assembly employing BaSO$_4$ as the reference sample. The photolominance (PL) spectra were collected with a spectrofluorophotometer (Shimadzu, RF-5301) using a Xe lamp as an excitation source with the excitation wavelength of 325 nm at room temperature. Before UV-Vis DRS, and FTIR measurements, the samples were freeze-dried in lyophilizerfor 24 h.

2.5 Photocatalytic activity of Ag$_2$O and Ag$_2$O-SPB

The photocatalytic activity of Ag$_2$O was measured in terms of the degradation of MB under visible-irradiation. The visible light was provided by a 300 W Xenon (Perfect Light, China) with a UV-cut filter ($\lambda \geq 400$ nm). All the experiments were conducted at ambient pressure and temperature. The distance between the lamp and the reactor was 10 cm for each experiment. For a typical run, 1 ml Ag$_2$O composite particle dispersion (0.1 wt% solid content) and 20 ml of 10 mg/l aqueous solution of MB were mixed together in a quartz glass reactor with stirring. This dispersion was stored in the dark for ca. 30 min prior to irradiation to establish the adsorption/desorption equilibrium of the dye on the catalyst surface. After a given time interval, the change in concentration was recorded as C/C_0 where C_0 was the initial concentration of MB aqueous solution, and C was the concentration at any given time (t).

3 Results and discussion

3.1 Synthesis of Ag$_2$O on the SPB

Narrow size distributed SPB was synthesized by photo-emulsion polymerization as confirmed by DLS. The mean diameter of PS core was about 80 nm while it was around 405 nm for SPB (Figure 2). For the preparation of Ag$_2$O-SPB through the chemical precipitation method, NaOH was added slowly so that well-dispersed particles were obtained. PAA brushes attached onto the PS core are
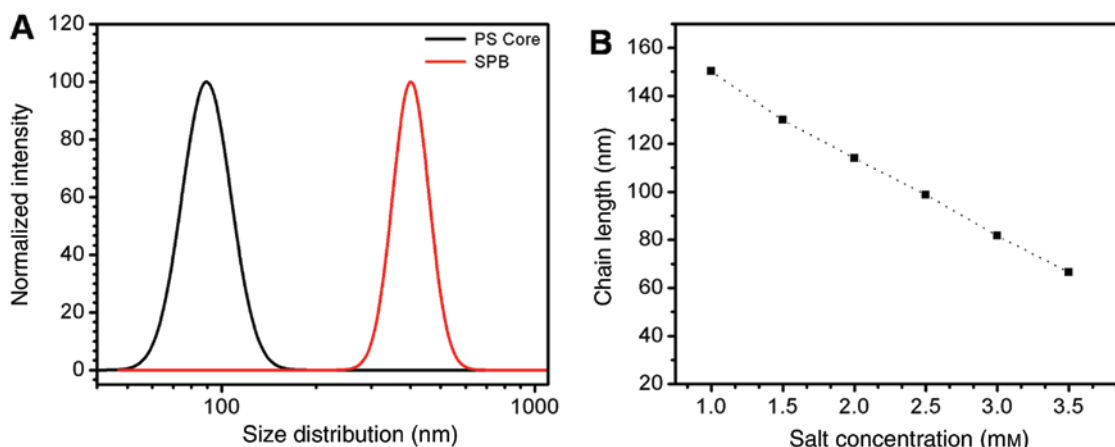
Figure 2: (A) Size distribution of PS core and PS-PAA SPB as measured by dynamic light scattering (DLS). (B) Effect of silver salt concentration on the chain length of polyelectrolyte brushes.

annealed brushes. It means that they are responsive to the ionic strength. It can be seen from Figure 2 that the chains of the PAA brushes had changed with different concentrations of silver salt. As we increased the concentration of salt, the chain length of brushes decreased substantially. This study helped in choosing the optimum concentration for silver salt.

TEM was used to observe the morphology of the pure SPB and Ag$_2$O immobilized in SPB. Figure 3A and B showed the TEM images of Ag$_2$O-SPB. It was observed from the TEM that Ag$_2$O NPs were successfully immobilized on the SPB after the precipitation reaction between AgNO$_3$ and NaOH. The average size of Ag$_2$O NPs was around 10 nm. Figure 3C showed that both the size and size distribution of Ag$_2$O-SPB increased compared with SPB as observed by DLS. It reflected that the counter ions of Ag$^+$ in SPB were reduced due to the reaction. The reduction of screening effect by counter ions will lead to the expanding of SPB, while slight aggregation of SPB may result during the reaction.

In order to investigate how Ag$_2$O NPs were immobilized on the SPB, one possible reason for this may be the preferential association of Ag$_2$O with the carboxylic groups (COO$^-$) present on the polyelectrolyte brush chains (35). The Ag$_2$O precursor was chemically co-precipitated directly in the brush layer. The generated silver oxide NPs within 10 nm were bound by the carboxyl groups and stabilized by the polymer chains in SPB.

It has been assumed that the COO$^-$ group of PAA on SPB has good co-ordination with silver NPs and that is why they are stable SPB (35). The coordination of functional group of PAA and Ag$_2$O might provide the good stability of the formed NPs. FTIR spectra of SPB without Ag$_2$O loading and with Ag$_2$O NPs immobilization on the SPB are shown in Figure 4. A strong absorption at 1710 cm^{-1} was observed which was derived from the C=O stretch in carboxyl groups in PAA brush. When Ag$_2$O NPs were formed, absorption of C=O stretch at 1710 cm^{-1} decreased, the absorption of symmetric (COO$^-$) stretch was enhanced at
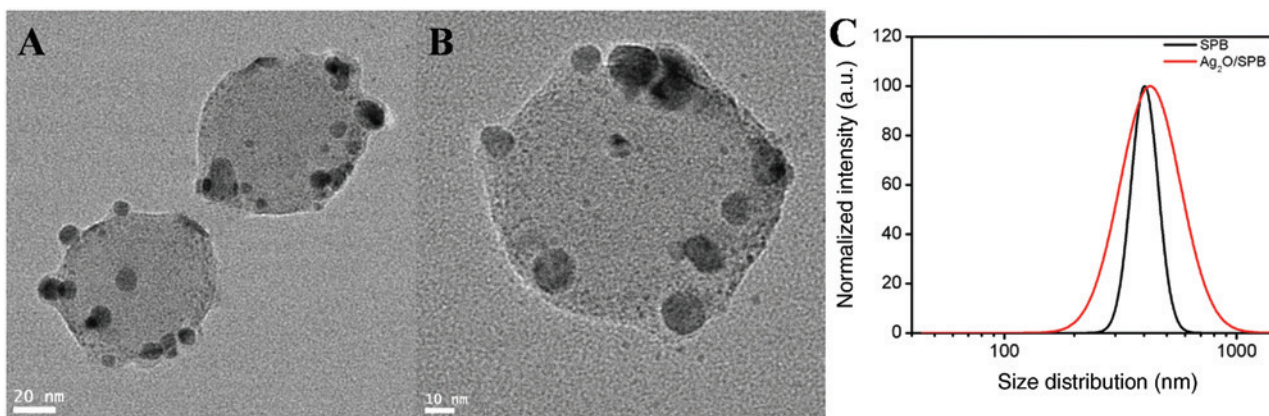
Figure 3: TEM images of (A & B) Ag$_2$O-SPB composite, and (C) DLS data of pure SPB and Ag$_2$O-SPB composite.
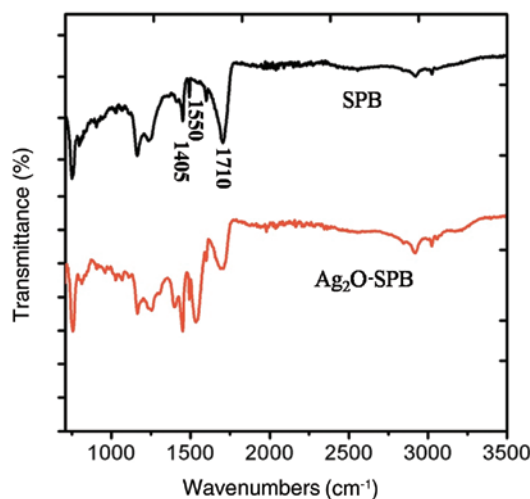
Figure 4: FTIR spectra of pure SPB, and Ag_2O-SPB composite.

Figure 6: Photoluminescence spectra of as prepared SPB, and Ag_2O-SPB composite.

1405 cm^{-1}, and a new absorption appeared at 1550 cm^{-1} from the asymmetric (COO$^-$) stretch (42). Free carboxyl groups (1710 cm^{-1}) still existed after the loading of Ag_2O NPs. These changes in FTIR spectra may reflect in part the coordination of carboxyl groups in PAA the Ag_2O.

The optical absorption properties of SPB and Ag_2O-SPB were investigated by UV-visible diffuse reflectance spectra as shown in Figure 5. Compared to SPB, Ag_2O-SPB showed much higher absorption in the visible range, which should be significantly activated in the visible light.

The PL spectra of SPB and the Ag_2O-SPB with an excitation wavelength of 325 nm are shown in Figure 6. There was no significant peak of pure SPB in the visible region, which is due to its non-conductive behavior. The wide peak of Ag_2O-SPB in the visible range implied that Ag_2O was present in SPB and its photoluminescence at around 450 nm.
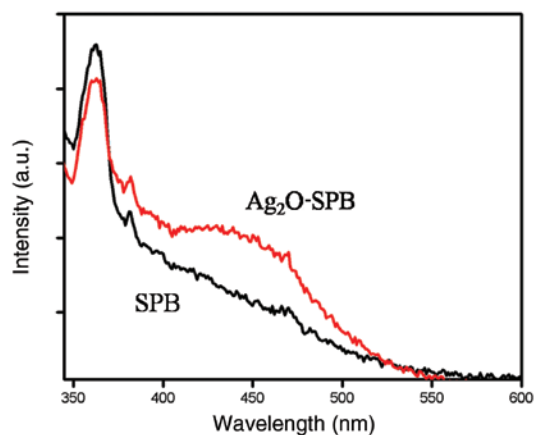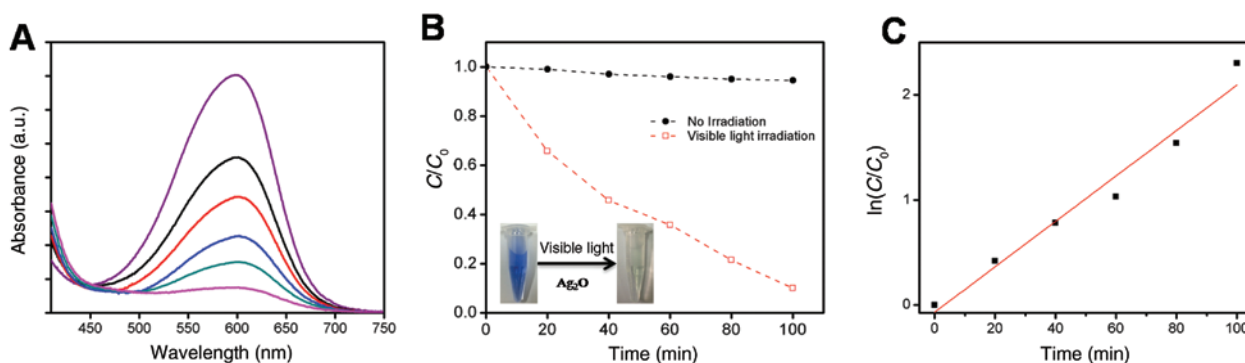
3.2 Photocatalytic activity of Ag_2O-SPB composite

Photocatalytic activity and reaction kinetics of Ag_2O-SPB were observed during the degradation of MB using visible light as shown in Figure 7. We had determined photocatalytic activity of composite in dark and in visible light for the comparison. After a specific time interval under visible light, the intensity of the peak at 600 nm, which is related to the characteristic UV-Vis absorption of the MB molecule, had decreased stepwise and disappeared after around 1.5 h which is shown in Figure 7A. We observed from Figure 7B that there was almost negligible degradation of MB in the dark because Ag_2O catalyst was only active in the visible range. Around 70% degradation of MB was achieved within 1 h of the photocatalytic reaction. The kinetics of MB degradation under visible light can be described by pseudo first order reaction

$$\ln\left(\frac{C_0}{C}\right) = kt$$

where k is the rate constant, C_0 and C are initial and concentration at given degradation time t, respectively. We plotted the graph of $\ln(C_0/C)$ as a function of t (Figure 7C). The graph for Ag_2O-SPB fitted linearly where the correlation coefficient value of R^2 was 0.9607. The calculated value of rate constant k was 0.021 min^{-1}, which showed the high catalytic activity of Ag_2O-SPB.

When Ag_2O-SPB composites were irradiated in the presence of visible light, electrons were produced in the conduction band while holes were produced in valence bands (Figure 8). During the irradiation, Ag might be

Figure 5: UV-visible diffuse reflectance spectra of Pure SPB, and Ag_2O-SPB composite.

Figure 7: (A) UV-Vis spectra of the degradation of MB in the presence of Ag$_2$O-SPB composite, (B) photocatalytic degradation of methyl blue and (C) kinetics of as prepared Ag$_2$O-SPB composite.
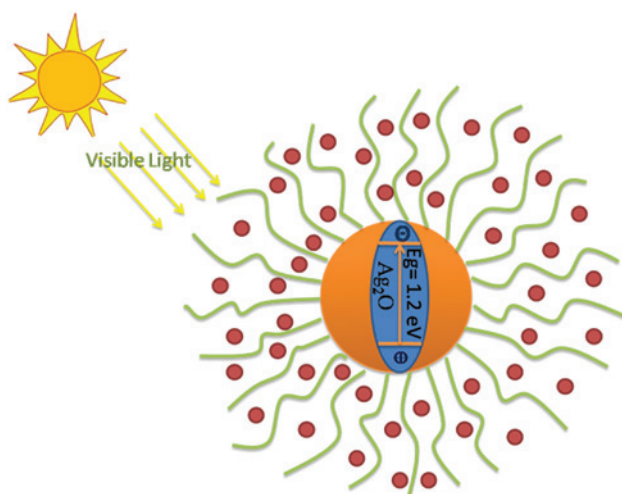
Figure 8: Proposed mechanism for degradation of MB.

formed by partial decomposition of Ag$_2$O attached on to SPB (26). Formation of Ag by *in-situ* photo generation made Ag$_2$O more stable (43).

4 Conclusions

We have demonstrated the successful synthesis of the visible light photocatalyst Ag$_2$O with the help of SPB as ideal nano-reactors. As observed by TEM, the Ag$_2$O NPs showed well-defined spherical structures with a size around 10 nm. UV-Vis diffuse reflectance and photoluminescence spectra were used to confirm the optical property of Ag$_2$O-SPB, which showed absorption and emission peaks in the visible range, respectively. The composite NPs of Ag$_2$O-SPB showed high photocatalytic activity in the degradation of dye MB under the visible light. This stable dispersion of Ag$_2$O-SPB is envisioned to

be used in the applications of dye wastewater treatment under visible photcatalysis.

References

1. Wahab R, Tripathy SK, Shin HS, Mohapatra M, Musarrat J, Al-Khedhairy AA, Kaushik NK. Photocatalytic oxidation of acetaldehyde with ZnO-quantum dots. Chem Eng J. 2013;226:154–60.
2. Ma SS, Xue JJ, Zhou YM, Zhang ZW. Photochemical synthesis of ZnO/Ag2O heterostructures with enhanced ultraviolet and visible photocatalytic activity. J Mater Chem A. 2014;2(20):7272–80.
3. Mahmoud MA, Qian W, El-Sayed MA. Following charge separation on the nanoscale in Cu2O-Au nanoframe hollow nanoparticles. Nano Lett. 2011;11(8):3285–9.
4. Yamazaki S, Fujiwara Y, Yabuno S, Adachi K, Honda K. Synthesis of porous platinum-ion-doped titanium dioxide and the photocatalytic degradation of 4-chlorophenol under visible light irradiation. Appl Catal B-Environ. 2012;121:148–53.
5. Tang J, Zou Z, Ye J. Efficient photocatalytic decomposition of organic contaminants over CaBi2O4 under visible-light irradiation. Angew Chem-Int Ed. 2004;43(34):4463–6.
6. Ji ZY, Shen XP, Yang JL, Xu YL, Zhu GX, Chen KM. Graphene oxide modified Ag2O nanocomposites with enhanced photocatalytic activity under visible-light irradiation. Eur J Inorg Chem. 2013;2013(36):6119–25.
7. Kisch H. Semiconductor photocatalysis—mechanistic and synthetic aspects. Angew Chem-Int Ed. 2013;52(3):812–47.
8. Habisreutinger SN, Schmidt-Mende L, Stolarczyk JK. Photocatalytic reduction of CO2 on TiO2 and other semiconductors. Angew Chem-Int Ed. 2013;52(29):7372–408.
9. Kim HI, Moon GH, Monllor-Satoca D, Park Y, Choi W. Solar photoconversion using graphene/TiO2 composites: nanographene

shell on TiO2 core versus TiO2 nanoparticles on graphene sheet. J Phys Chem C. 2012;116(1):1535–43.

10. Shul Y, Kim H, Haam S, Han H. Photocatalytic characteristics of TiO2 supported on SiO2. Res Chem Intermed. 2003;29 (7–9):849–59.

11. Zhuang SD, Xu XY, Pang YR, Hu JG, Yang C, Tong L, Zhou. YX PEGME-bonded SnO2 quantum dots for excellent photocatalytic activity. Rsc Adv. 2013;3(43):20422–8.

12. Wang G, Huang BB, Wang L, Wang ZY, Lou ZZ, Qin XY, Zhang XY, Dai, Y. CuO/CuSCN valence state heterojunctions with visible light enhanced and ultraviolet light restrained photocatalytic activity. Chem Comm. 2014;50(29):3814–6.

13. Wang WZ, Wang LJ, Shi HL, Liang YJ. A room temperature chemical route for large scale synthesis of sub-15 nm ultralong CuO nanowires with strong size effect and enhanced photocatalytic activity. Crystengcomm. 2012;14(18):5914–22.

14. Tian CG, Zhang Q, Wu AP, Jiang MJ, Liang ZL, Jiang BJ, Fu HG. Cost-effective large-scale synthesis of ZnO photocatalyst with excellent performance for dye photodegradation. Chem Comm. 2012;48(23):2858–60.

15. Yang YF, Li YG, Zhu LP, He HP, Hu L, Huang JY, Hu F, He B, Ye Z. Shape control of colloidal Mn doped ZnO nanocrystals and their visible light photocatalytic properties. Nanoscale 2013;5(21):10461–71.

16. Zhao K, Wu Z, Jiang Y. Synthesis, characterization, and optical properties of a flower-like zinc oxide microstructure. Res Chem Intermed. 2015;41(6):3401–8.

17. Zan X, Su Z. Incorporation of nanoparticles into polyelectrolyte multilayers via counterion exchange and in situ reduction. Langmuir 2009;25(20):12355–60.

18. Zhang X, Zan X, Su Z. Polyelectrolyte multilayer supported Pt nanoparticles as catalysts for methanol oxidation. J Mater Chem. 2011;21(44):17783–9.

19. Zhang X, Su Z. Polyelectrolyte-multilayer-supported Au@Ag core-shell nanoparticles with high catalytic activity. Adv Mater. 2012;24(33):4574–7.

20. Pastrana-Martinez LM, Morales-Torres S, Kontos AG, Moustakas NG, Faria JL, Dona-Rodriguez JM. TiO2, surface modified TiO2 and graphene oxide-TiO2 photocatalysts for degradation of water pollutants under near-UV/Vis and visible light. Chem Eng J. 2013;224:17–23.

21. Kim J, Choi W. TiO2 modified with both phosphate and platinum and its photocatalytic activities. Appl Catal B-Environ. 2011;106(1–2):39–45.

22. Liu S, Guo EY, Yin LW. Tailored visible-light driven anatase TiO2 photocatalysts based on controllable metal ion doping and ordered mesoporous structure. J Mater Chem. 2012;22(11):5031–41.

23. An L, Wang G, Cheng Y, Zhao L, Gao F, Tian Y. Ultrasonic-assisted synthesis of visible-light-driven TiO2/Bi2O3 nanocomposite photocatalysts: characterization, properties and azo dye removal application. Res Chem Intermed. 2014;41:1–13.

24. Sahoo C, Gupta AK. Optimization of photocatalytic degradation of methyl blue using silver ion doped titanium dioxide by combination of experimental design and response surface approach. J Hazard Mater. 2012;215–216: 302–10.

25. Wu M, Yan J-M, Zhao M, Jiang Q. Facile synthesis of an Ag2O–ZnO nanohybrid and its high photocatalytic activity. ChemPlusChem. 2012;77(10):931–5.

26. Wang X, Li S, Yu H, Yu J, Liu S. Ag2O as a new visible-light photocatalyst: self-stability and high photocatalytic activity. Chem Euro J. 2011;17(28):7777–80.

27. Xu M, Han L, Dong S. Facile fabrication of highly efficient g-C3N4/Ag2O heterostructured photocatalysts with enhanced visible-light photocatalytic activity. ACS Appl Mater Inter. 2013;5(23):12533–40.

28. Bugarčić ZM, Divac VM, Gavrilović MP. An efficient route to phenylselenoethers in the presence of Ag2O. Monatshefte für Chemie–Chem Monthly. 2007;138(10):985–8.

29. Ida Y, Watase S, Shinagawa T, Watanabe M, Chigane M, Inaba M, Tasaka, A, Izaki M. Direct electrodeposition of 1.46 eV Bandgap Silver(I) oxide semiconductor films by electrogenerated acid. Chem Mater. 2008;20(4):1254–6.

30. Wang X, Wu H-F, Kuang Q, Huang R-B, Xie Z-X, Zheng L-S. Shape-dependent antibacterial activities of Ag2O polyhedral particles. Langmuir 2009;26(4):2774–8.

31. Sarkar D, Ghosh CK, Mukherjee S, Chattopadhyay KK. Three dimensional Ag2O/TiO2 type-II (p–n) nanoheterojunctions for superior photocatalytic activity. ACS Appl Mater Inter. 2012;5(2):331–7.

32. Lyu L-M, Huang MH. Investigation of relative stability of different facets of Ag2O nanocrystals through face-selective etching. J Phys Chem C. 2011;115(36):17768–73.

33. Wang G, Ma XC, Huang BB, Cheng HF, Wang ZY, Zhan J, Qin XY, Zhang XY, Dai, Y. Controlled synthesis of Ag2O microcrystals with facet-dependent photocatalytic activities. J Mater Chem. 2012;22(39):21189–94.

34. Studart AR, Amstad E, Gauckler LJ. Colloidal stabilization of nanoparticles in concentrated suspensions. Langmuir 2006;23(3):1081–90.

35. Zhu Y, Chen K, Wang X, Guo X. Spherical polyelectrolyte brushes as a nanoreactor for synthesis of ultrafine magnetic nanoparticles. Nanotechnology 2012;23(26):265601.

36. Guo X, Weiss A, Ballauff M. Synthesis of spherical polyelectrolyte brushes by photoemulsion polymerization. Macromolecules 1999;32(19):6043–6.

37. Ballauff M. Spherical polyelectrolyte brushes. Prog Poly Sci. 2007;32(10):1135–51.

38. Guo X, Ballauff M. Spatial dimensions of colloidal polyelectrolyte brushes as determined by dynamic light scattering. Langmuir 2000;16(23):8719–26.

39. Ahmad A, Liu X, Li L, Guo X. Chapter four – progress in polymer nanoreactors: spherical polyelectrolyte brushes. In: Guy BM, editor. Adv Chem Eng: vol. 44: New York, NY, USA: Elsevier; Academic Press; 2014. pp. 193–225.

40. Schrinner M, Proch S, Mei Y, Kempe R, Miyajima N, Ballauff M. Stable bimetallic gold-platinum nanoparticles immobilized on spherical polyelectrolyte brushes: synthesis, characterization, and application for the oxidation of alcohols. Adv Mater. 2008;20(10):1928–33.

41. Liu J, Wang J, Zhu Z, Li L, Guo X, Lincoln SF, Prud'homme RK. Cooperative catalytic activity of cyclodextrin and Ag nanoparticles immobilized on spherical polyelectrolyte brushes. Aiche J. 2014;60(6):1977–82.

42. Kirwan LJ, Fawell PD, van Bronswijk W. In situ FTIR-ATR examination of poly(acrylic acid) adsorbed onto hematite at low pH. Langmuir 2003;19(14):5802–7.

43. Kuai L, Geng B, Chen X, Zhao Y, Luo Y. Facile subsequently light-induced route to highly efficient and stable sunlight-driven Ag-AgBr plasmonic photocatalyst. Langmuir 2010;26(24):18723–7.